Provided for non-commercial research and education use.
Not for reproduction, distribution or commercial use.

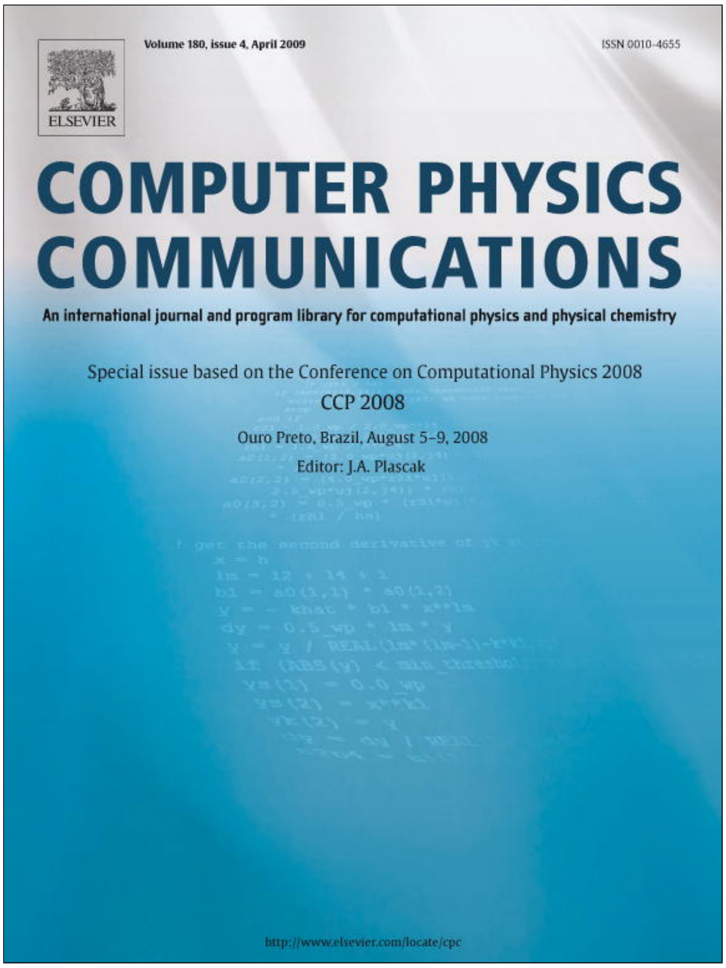

Volume 180, issue 4, April 2009
ISSN 0010-4655

COMPUTER PHYSICS COMMUNICATIONS

An international journal and program library for computational physics and physical chemistry

Special issue based on the Conference on Computational Physics 2008
CCP 2008
Ouro Preto, Brazil, August 5–9, 2008
Editor: J.A. Plascak

http://www.elsevier.com/locate/cpc

This article appeared in a journal published by Elsevier. The attached copy is furnished to the author for internal non-commercial research and education use, including for instruction at the authors institution and sharing with colleagues.

Other uses, including reproduction and distribution, or selling or licensing copies, or posting to personal, institutional or third party websites are prohibited.

In most cases authors are permitted to post their version of the article (e.g. in Word or Tex form) to their personal website or institutional repository. Authors requiring further information regarding Elsevier's archiving and manuscript policies are encouraged to visit:

http://www.elsevier.com/copyright

Computer Physics Communications 180 (2009) 497–502

Contents lists available at ScienceDirect

Computer Physics Communications

www.elsevier.com/locate/cpc

Cluster Monte Carlo and numerical mean field analysis for the water liquid–liquid phase transition

Marco G. Mazza [a,*], Kevin Stokely [a], Elena G. Strekalova [a], H. Eugene Stanley [a], Giancarlo Franzese [b]

[a] Center for Polymer Studies and Department of Physics, Boston University, Boston, MA 02215, USA
[b] Departament de Fisica Fonamental, Universitat de Barcelona, Diagonal 647, 08028 Barcelona, Spain

ARTICLE INFO

Article history:
Received 25 October 2008
Received in revised form 15 January 2009
Accepted 19 January 2009
Available online 22 January 2009

PACS:
61.20.Ja
61.20.Gy

Keywords:
Wolff algorithm
Liquid–liquid phase transitions

ABSTRACT

Using Wolff's cluster Monte Carlo simulations and numerical minimization within a mean field approach, we study the low temperature phase diagram of water, adopting a cell model that reproduces the known properties of water in its fluid phases. Both methods allow us to study the thermodynamic behavior of water at temperatures, where other numerical approaches – both Monte Carlo and molecular dynamics – are seriously hampered by the large increase of the correlation times. The cluster algorithm also allows us to emphasize that the liquid–liquid phase transition corresponds to the percolation transition of tetrahedrally ordered water molecules.

Published by Elsevier B.V.

1. Introduction

Water is possibly the most important liquid for life [1] and, at the same time, is a very peculiar liquid [2]. In the stable liquid regime its thermodynamic response functions behave qualitatively differently than a typical liquid. The isothermal compressibility K_T, for example, has a minimum as a function of temperature at $T = 46\,^\circ\mathrm{C}$, while for a typical liquid K_T monotonically decreases upon cooling. Water's anomalies become even more pronounced as the system is cooled below the melting point and enters the metastable supercooled regime [3].

Different hypotheses have been proposed to rationalize the anomalies of water [4]. All these interpretations, but one, predict the existence of a liquid–liquid phase transition in the supercooled state, consistent with the experiments to date [4] and supported by different models [2].

To distinguish among the different interpretations, many experiments have been performed [5]. However, the freezing in the temperature range of interest can be avoided only for water in confined geometries or on the surface of macromolecules [4,6]. Since experiments in the supercooled region are difficult to perform, numerical simulations have played an important role in recent years to help interpret the data. However, also the simulations at very low temperature T are hampered by the glassy dynamics of the empirical models of water [7,8]. For these reasons it is important to implement more efficient numerical simulations for simple models, able to capture the fundamental physics of water but also less computationally expensive. Here we introduce the implementation of a Wolff cluster algorithm [9] for the Monte Carlo (MC) simulations of a cell model for water [10]. The model is able to reproduce all the different scenarios proposed to interpret the behavior of water [11] and has been analyzed (i) with mean field (MF) [10,12,13], (ii) with Metropolis MC simulations [8,14] and (iii) with Wang–Landau MC density of state algorithm [15]. Recent Metropolis MC simulations [8] have shown that very large times are needed to equilibrate the system as $T \to 0$, as a consequence of the onset of the glassy dynamics. The implementation of the Wolff clusters MC dynamics, presented here, allows us to (i) drastically reduce the equilibration times of the model at very low T and (ii) give a geometrical characterization of the regions of correlated water molecules (clusters) at low T and show that the liquid–liquid phase transition can be interpreted as a percolation transition of the tetrahedrally ordered clusters.

2. The model

The system consists of N particles distributed within a volume V in d dimensions. The volume is divided into N cells of volume v_i with $i \in [1, N]$. For sake of simplicity, these cells are chosen of the same size, $v_i = V/N$, but the generalization to the case in which the volume can change without changes in the topology of the nearest-neighbor (n.n.) is straightforward. By definition,

---

[*] Corresponding author.
E-mail address: marcokyb@bu.edu (M.G. Mazza).

0010-4655/$ – see front matter Published by Elsevier B.V.
doi:10.1016/j.cpc.2009.01.018

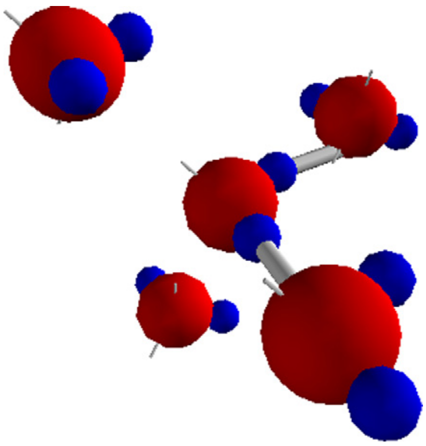

Fig. 1. A pictorial representation of five water molecules in $3d$. Two hydrogen bonds (grey links) connect the hydrogens (in blue) of the central molecule with the lone electrons (small gray lines) of two nearest neighbor (n.n.) molecules. A bond index (arm) with $q = 6$ possible values is associated to each hydrogen and lone electron, giving rise to q^4 possible orientational states for each molecule. A hydrogen bond can be formed only if the two facing arms of the n.n. molecules are in the same state. Arms on the same molecule interact among themselves to mimic the O–O–O interaction that drives the molecules toward a tetrahedral local structure. (For interpretation of the references to color in this figure legend, the reader is referred to the web version of this article.)

$v_i \geqslant v_0$, where v_0 is the molecule hard-core volume. Each cell has a variable $n_i = 0$ for a gas-like or $n_i = 1$ for a liquid-like cell. We partition the total volume in a way such that each cell has at least four n.n. cells, e.g., as in a cubic lattice in $3d$ or a square lattice in $2d$. Periodic boundary conditions are used to limit finite-size effects.

The system is described by the Hamiltonian [10]

$$\mathscr{H} = -\epsilon \sum_{\langle i,j\rangle} n_i n_j - J \sum_{\langle i,j\rangle} n_i n_j \delta_{\sigma_{ij},\sigma_{ji}} - J_\sigma \sum_i n_i \sum_{(k,l)_i} \delta_{\sigma_{ik},\sigma_{il}}, \qquad (1)$$

where $\epsilon > 0$ is the strength of the van der Waals attraction, $J > 0$ accounts for the hydrogen bond energy, with four (Potts) variables $\sigma_{ij} = 1, \ldots, q$ representing bond indices of molecule i with respect to the four n.n. molecules j, $\delta_{a,b} = 1$ if $a = b$ and $\delta_{a,b} = 0$ otherwise, and $\langle i, j\rangle$ denotes that i and j are n.n. The model does not assume a privileged state for bond formation. Any time two facing bond indices (arms) are in the same (Potts) state, a bond is formed. The third term represents an intramolecular (IM) interaction accounting for the O–O–O correlation [16], locally driving the molecules toward a tetrahedral configuration. When the bond indices of a molecule are in the same state, the energy is decreased by an amount $J_\sigma \geqslant 0$ and we associate this local ordered configuration to a local tetrahedral arrangement [17]. The notation $(k,l)_i$ indicates one of the six different pairs of the four bond indices of molecule i (Fig. 1).

Experiments show that the formation of a hydrogen bond leads to a local volume expansion [2]. Thus in our system the total volume is

$$V = N v_0 + N_{HB} v_{HB}, \qquad (2)$$

where

$$N_{HB} \equiv \sum_{\langle i,j\rangle} n_i n_j \delta_{\sigma_{ij},\sigma_{ji}} \qquad (3)$$

is the total number of hydrogen bonds, and v_{HB} is the constant specific volume increase due to the hydrogen bond formation.

3. Mean-field analysis

In the mean-field (MF) analysis the macrostate of the system in equilibrium at constant pressure P and temperature T (NPT ensemble) may be determined by a minimization of the Gibbs free energy per molecule, $g \equiv (\langle\mathscr{H}\rangle + PV - TS)/N_w$, where

$$N_w = \sum_i n_i \qquad (4)$$

is the total number of liquid-like cells, and $S = S_n + S_\sigma$ is the sum of the entropy S_n over the variables n_i and the entropy S_σ over the variables σ_{ij}.

A MF approach consists of writing g explicitly using the approximations

$$\sum_{\langle i,j\rangle} n_i n_j \to 2Nn^2, \qquad (5)$$

$$\sum_{\langle i,j\rangle} n_i n_j \delta_{\sigma_{ij},\sigma_{ji}} \to 2Nn^2 p_\sigma, \qquad (6)$$

$$\sum_i n_i \sum_{(k,l)_i} \delta_{\sigma_{ik},\sigma_{il}} \to 6Nnp_\sigma, \qquad (7)$$

where $n = N_w/N$ is the average of n_i, and p_σ is the probability that two adjacent bond indices σ_{ij} are in the appropriate state to form a hydrogen bond.

Therefore, in this approximation we can write

$$V = Nv_0 + 2Nn^2 p_\sigma v_{HB}, \qquad (8)$$

$$\langle\mathscr{H}\rangle = -2\big[\epsilon n + (Jn + 3J_\sigma)p_\sigma\big]nN. \qquad (9)$$

The probability p_σ, properly defined as the thermodynamic average over the whole system, is approximated as the average over two neighboring molecules, under the effect of the mean-field h of the surrounding molecules

$$p_\sigma = \langle\delta_{\sigma_{ij},\sigma_{ji}}\rangle_h. \qquad (10)$$

The ground state of the system consists of all N variables $n_i = 1$, and all σ_{ij} in the same state. At low temperatures, the symmetry will remain broken, with the majority of the σ_{ij} in a preferred state. We associate this preferred state to the tetrahedral order of the molecules and define m_σ as the density of the bond indices in the tetrahedral state, with $0 \leqslant m_\sigma \leqslant 1$. Therefore, the number density n_σ of bond indices σ_{ij} in the tetrahedral state is

$$n_\sigma = \frac{1 + (q-1)m_\sigma}{q}. \qquad (11)$$

Since an appropriate form for h is [10]

$$h = 3J_\sigma n_\sigma, \qquad (12)$$

we obtain that $\frac{3J_\sigma}{q} \leqslant h \leqslant 3J_\sigma$.

The MF expressions for the entropies S_n of the N variables n_i, and S_σ of the $4Nn$ variables σ_{ij}, are then [12]

$$S_n = -k_B N\big(n\log(n) + (1-n)\log(1-n)\big), \qquad (13)$$

$$S_\sigma = -k_B 4Nn\big[n_\sigma \log(n_\sigma) + (1-n_\sigma)\log(1-n_\sigma) + \log(q-1)\big], \qquad (14)$$

where k_B is the Boltzmann constant.

Equating

$$p_\sigma \equiv n_\sigma^2 + \frac{(1-n_\sigma)^2}{q-1}, \qquad (15)$$

with the approximate expression in Eq. (10), allows for solution of n_σ, and hence g, in terms of the order parameter m_σ and n.

By minimizing numerically the MF expression of g with respect to n and m_σ, we find the equilibrium values $n^{(eq)}$ and $m_\sigma^{(eq)}$ and, with Eqs. (4) and (2), we calculate the density ρ at any (T, P) and the full equation of state. An example of minimization of g is

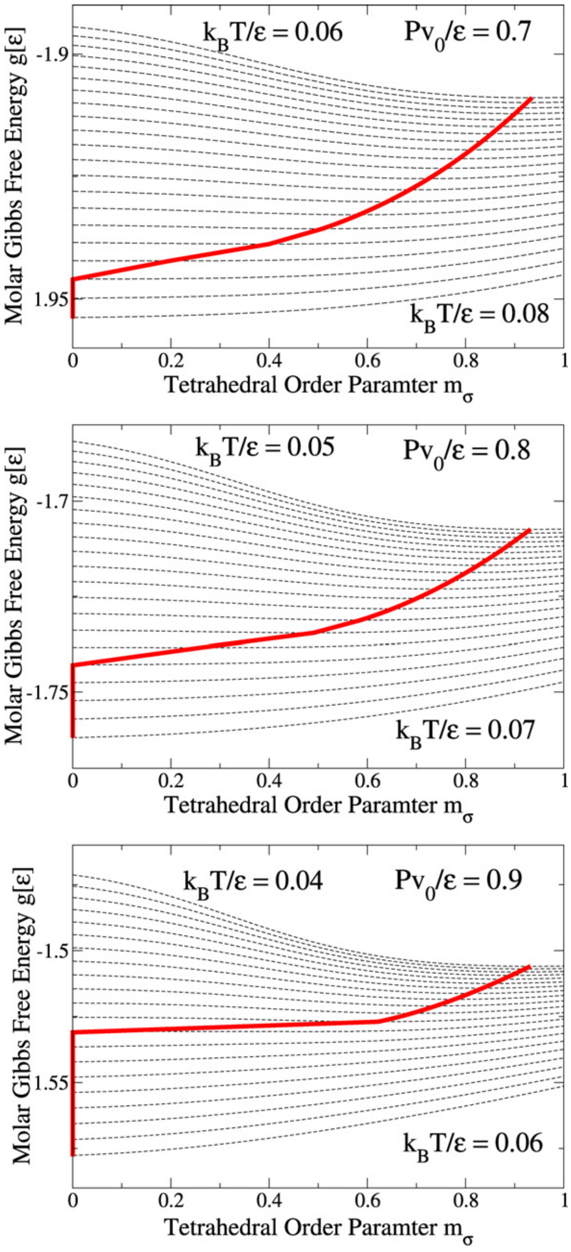

Fig. 2. Numerical minimization of the molar Gibbs free energy g in the mean field approach. The model's parameters are $J/\epsilon = 0.5$, $J_\sigma/\epsilon = 0.05$, $v_{HB}/v_0 = 0.5$ and $q = 6$. In each panel we present g (dashed lines) calculated at constant P and different values of T. The thick line crossing the dashed lines connects the minima $m_\sigma^{(eq)}$ of g at different T. Upper panel: $Pv_0/\epsilon = 0.7$, for T going from $k_BT/\epsilon = 0.06$ (top) to $k_BT/\epsilon = 0.08$ (bottom). Middle panel: $Pv_0/\epsilon = 0.8$, for T going from $k_BT/\epsilon = 0.05$ (top) to $k_BT/\epsilon = 0.07$ (bottom). Lower panel: $Pv_0/\epsilon = 0.9$, for T going from $k_BT/\epsilon = 0.04$ (top) to $k_BT/\epsilon = 0.06$ (bottom). In each panel dashed lines are separated by $k_B\delta T/\epsilon = 0.001$. In all the panels $m_\sigma^{(eq)}$ increases when T decreases, being 0 (marking the absence of tetrahedral order) at the higher temperatures and $\simeq 0.9$ (high tetrahedral order) at the lowest temperature. By changing T, $m_\sigma^{(eq)}$ changes in a continuous way for $Pv_0/\epsilon = 0.7$ and 0.8, but discontinuous for $Pv_0/\epsilon = 0.9$ and higher P.

presented in Fig. 2 where, for the model's parameters $J/\epsilon = 0.5$, $J_\sigma/\epsilon = 0.05$, $v_{HB}/v_0 = 0.5$, $q = 6$, a discontinuity in $m_\sigma^{(eq)}$ is observed for $Pv_0/\epsilon > 0.8$. As discussed in Refs. [10,14] this discontinuity corresponds to a first order phase transition between two liquid phases with different degree of tetrahedral order and, as a consequence, different density. The higher P, at which the change in $m_\sigma^{(\mathrm{eq})}$ is continuous, corresponds to the pressure of a liquid–liquid critical point (LLCP). The occurrence of the LLCP is consistent with one of the possible interpretations of the anomalies of water, as discussed in Ref. [12]. However, for different choices of parameters, the model reproduces also the other proposed scenarios [11].

4. The simulation with the Wolff's clusters Monte Carlo algorithm

To perform MC simulations in the *NPT* ensemble, we consider a modified version of the model in which we allow for continuous volume fluctuations. To this goal, (i) we assume that the system is homogeneous with all the variables n_i set to 1 and all the cells with volume $v = V/N$; (ii) we consider that $V \equiv V_{MC} + N_{HB}v_{HB}$, where $V_{MC} \geqslant Nv_0$ is a dynamical variable allowed to fluctuate in the simulations; (iii) we replace the first (van der Waals) term of the Hamiltonian in Eq. (1) with a Lennard-Jones potential with attractive energy $\epsilon > J$ and with a hard-core at distance r_0

$$U_W(r) \equiv \begin{cases} \infty & \text{if } r \leqslant r_0,\\ \epsilon\left[\left(\frac{r_0}{r}\right)^{12} - \left(\frac{r_0}{r}\right)^{6}\right] & \text{if } r > r_0, \end{cases} \tag{16}$$

where $r_0 \equiv (v_0)^{1/d}$ where d is set to 2 (2d case); the distance between two n.n. molecules is $(V/N)^{1/d}$, and the distance r between two generic molecules is the Cartesian distance between the center of the cells in which they are included.

The simplification (i) could be removed, by allowing the cells to assume different volumes v_i and keeping fixed the number of possible n.n. cells. However, the results of the model under the simplification (i) compares well with experiments [12]. Furthermore, the simplification (i) allows to drastically reduce the computational cost of the evaluation of the $U_W(r)$ term from $N(N-1)$ to $N-1$ operations. The changes (i)–(iii) modify the model used for the mean field analysis and allow off-lattice MC simulations for a cell model in which the topology of the molecules (i.e. the number of n.n.) is preserved. The comparison of the mean field results with the MC simulations show that these changes do not modify the physics of the system.

We perform MC simulations with $N = 2500$ and $N = 10000$ molecules, each with four n.n. molecules, at constant P and T, in 2d, and with the same parameters used for the mean field analysis. To each molecules we associate a cell on a square lattice. The Wolff algorithm is based on the definition of a cluster of variables chosen in such a way to be thermodynamically correlated [18,19]. To define the Wolff cluster, a bond index (arm) of a molecule is randomly selected; this is the initial element of a stack. The cluster is grown by first checking the remaining arms of the same initial molecule: if they are in the same Potts state, then they are added to the stack with probability $p_{\text{same}} \equiv 1 - \exp(-\beta J_\sigma)$ [9], where $\beta \equiv (k_BT)^{-1}$. This choice for the probability p_{same} depends on the interaction J_σ between two arms on the same molecule and guarantees that the connected arms are thermodynamically correlated [19]. Next, the arm of a new molecule, facing the initially chosen arm, is considered. To guarantee that connected facing arms correspond to thermodynamically correlated variables, is necessary [18] to link them with the probability $p_{\text{facing}} \equiv 1 - \exp(-\beta J')$ where $J' \equiv J - Pv_{HB}$ is the P-dependent effective coupling between two facing arms as results from the enthalpy $\mathscr{H} + PV$ of the system. It is important to note that J' can be positive or negative depending on P. If $J' > 0$ and the two facing arms are in the same state, then the new arm is added to the stack with probability p_{facing}; if $J' < 0$ and the two facing arms are in different states, then the new arm is added with probability p_{facing} [20]. Only after every possible direction of growth for the cluster has been considered the values of the arms are changed in a stochastic way; again we need to consider two cases: (i) if $J' > 0$, all arms are set to the same new value

$$\sigma^{\text{new}} = \left(\sigma^{\text{old}} + \phi\right) \bmod q, \tag{17}$$

where ϕ is a random integer between 1 and q; (ii) if $J' < 0$, the state of every single arm is changed (rotated) by the same random constant $\phi \in [1, \ldots q]$

$$\sigma_i^{\rm new} = \left(\sigma_i^{\rm old} + \phi\right) \bmod q. \tag{18}$$

In order to implement a constant P ensemble we let the volume fluctuate. A small increment $\Delta r/r_0 = 0.01$ is chosen with uniform random probability and added to the current radius of a cell. The change in volume $\Delta V \equiv V^{\rm new} - V^{\rm old}$ and van der Waals energy ΔE_W is computed and the move is accepted with probability $\min(1, \exp[-\beta(\Delta E_W + P\Delta V - T\Delta S)])$, where $\Delta S \equiv -Nk_B \ln(V^{\rm new}/V^{\rm old})$ is the entropic contribution.

5. Monte Carlo correlation times

The cluster MC algorithm described in the previous section turns out to be very efficient at low T, allowing to study the thermodynamics of deeply supercooled water with quite intriguing results [21]. To estimate the efficiency of the cluster MC dynamics with respect to the standard Metropolis MC dynamics, we evaluate in both dynamics, and compare, the autocorrelation function of the average magnetization per site $M_i \equiv \frac{1}{4}\sum_j \sigma_{ij}$, where the sum is over the four bonding arms of molecule i,

$$C_M(t) \equiv \frac{1}{N}\sum_i \frac{\langle M_i(t_0+t)M_i(t_0)\rangle - \langle M_i\rangle^2}{\langle M_i^2\rangle - \langle M_i\rangle^2}. \tag{19}$$

For sake of simplicity, we define the MC dynamics autocorrelation time τ as the time, measured in MC steps, when $C_M(\tau) = 1/e$. Here we define a MC step as $4N$ updates of the bond indices followed by a volume update, i.e. as $4N + 1$ steps of the algorithm.

In Fig. 3 we show a comparison of $C_M(t)$ for the Metropolis and Wolff algorithm implementations of this model for a system with $N = 50 \times 50$, at three temperatures along an isobar below the LLCP, and approaching the line of the maximum, but finite, correlation length, also known as Widom line $T_W(P)$ [12]. In the top panel, at $T \gg T_W(P)$ ($k_BT/\epsilon = 0.11$, $Pv_0/\epsilon = 0.6$), we find a correlation time for the Wolff's cluster MC dynamics $\tau_{\rm W} \approx 3 \times 10^3$, and for the Metropolis dynamics $\tau_{\rm M} \approx 10^6$. In the middle panel, at $T > T_W(P)$ ($k_BT/\epsilon = 0.09$, $Pv_0/\epsilon = 0.6$) the difference between the two correlation times is larger: $\tau_{\rm W} \approx 2.5 \times 10^3$, $\tau_{\rm M} \approx 3 \times 10^6$. The bottom panel, at $T \simeq T_W(P)$ ($k_BT/\epsilon = 0.06$, $Pv_0/\epsilon = 0.6$) shows $\tau_{\rm W} \approx 3.7 \times 10^2$, while $\tau_{\rm M}$ is beyond the accessible time window ($\tau_{\rm M} > 10^7$).

Since as $T \to 0$ the system enters a glassy state [8], the efficiency $\tau_{\rm M}/\tau_{\rm W}$ grows at lower T allowing the evaluation of thermodynamics averages even at $T \ll T_C$ [21]. In particular, the cluster MC algorithm turns out to be very efficient when approaching the Widom line in the vicinity of the LLCP, with an efficiency of the order of 10^4. We plan to analyze in a systematic way how the efficiency $\tau_{\rm M}/\tau_{\rm W}$ grows on approaching the LLCP. This result is well known for the standard liquid–gas critical point [9] and, on the basis of our results, could be extended also to the LLCP. However, this analysis is very expensive in terms of CPU time and goes beyond the goal of the present work. Nevertheless, the percolation analysis, presented in the next section, helps in understanding the physical reason for this large efficiency.

The efficiency is a consequence of the fact that the average size of Wolff's clusters changes with T and P in the same way as the average size of the regions of correlated molecules [19], i.e. a Wolff's cluster statistically represents a region of correlated molecules. Moreover, the mean cluster size diverges at the critical point with the same exponent of the Potts magnetic susceptibility [19], and the clusters percolate at the critical point, as we will discuss in the next section.

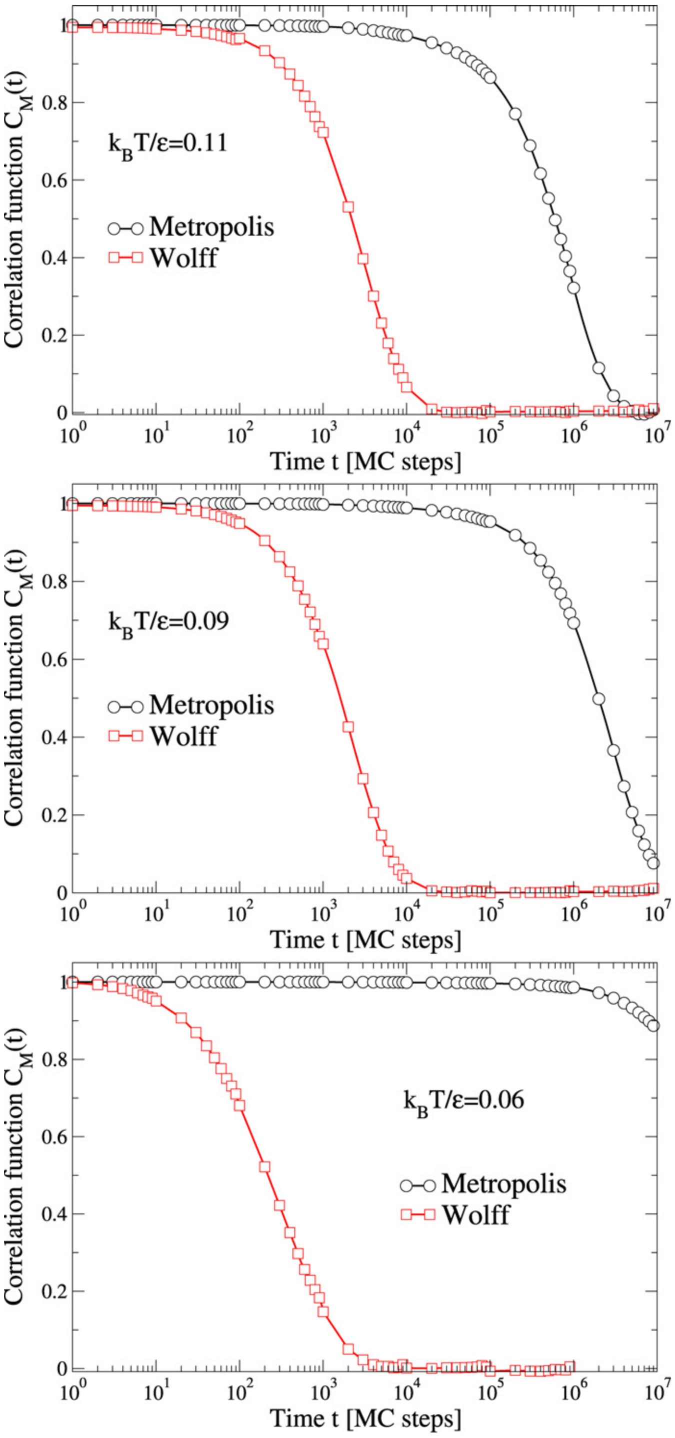

Fig. 3. Comparison of the autocorrelation function $C_M(t)$ for the Metropolis (circles) and Wolff (squares) implementation of the present model. We show the temperatures $k_BT/\epsilon = 0.11$ (top panel), $k_BT/\epsilon = 0.09$ (middle panel), $k_BT/\epsilon = 0.06$ (bottom panel), along the isobar $Pv_0/\epsilon = 0.6$ close to the LLCP for $N = 50 \times 50$.

6. Percolating clusters of correlated molecules

The efficiency of the Wolff cluster algorithm is a consequence of the exact relation between the average size of the finite clusters and the average size of the regions of thermodynamically correlated molecules. The proof of this relation at any T derives in a straightforward way from the proof for the case of Potts variables [19]. This relation allows one to identify the clusters built during the MC dynamics with the correlated regions and emphasizes (i) the appearance of heterogeneities in the structural correlations [22], and (ii) the onset of percolation of the clusters of tetrahedrally ordered molecules at the LLCP [23], as shown in Fig. 4.

A systematic percolation analysis [18] is beyond the goal of this report, however configurations such as those in Fig. 4 allow the following qualitative considerations. At $T > T_C$ the average cluster size is much smaller than the system size. Hence, the structural correlations among the molecules extends only to short distances. This suggests that the correlation time of a local dynamics, such as Metropolis MC or molecular dynamics, would be short on average at this temperature and pressure. Nevertheless, the system appears strongly heterogeneous with the coexistence of large and small clusters, suggesting that the distribution of correlation times evaluated among molecules at a given distance could be strongly heterogeneous. The clusters appear mostly compact but with a fractal surface, suggesting that borders between clusters can rapidly change.

At $T \simeq T_C$ there is one large cluster, in red on the right of the middle panel of Fig. 4, with a linear size comparable to the system linear extension and spanning in the vertical direction. The appearance of spanning clusters shows the onset of the percolation geometrical transition. At this state point the correlation time of local, such as Metropolis MC dynamics or molecular dynamics would be very slow as a consequence of the large extension of the structurally correlated region. On the other hand, the correlation time of the Wolff's cluster dynamics is short because it changes in one single MC step the state of all the molecules in clusters, some of them with very large size. Once the spanning cluster is formed, it breaks the symmetry of the system and a strong effective field acts on the molecules near its border to induce their reorientation toward a tetrahedral configuration with respect the molecules in the spanning cluster.

As shown in Fig. 4, the spanning cluster appears as a fractal object, with holes of any size. The same large distribution of sizes characterizes also the finite clusters in the system. The absence of a characteristic size for the clusters (or the holes of the spanning cluster) is the consequence of the fluctuations at any length-scale, typical of a critical point.

At $T < T_C$ the majority of the molecules belongs to a single percolating cluster that represents the network of tetrahedrally ordered molecules. All the other clusters are small, with a finite size that corresponds to the regions of correlated molecules. The presence of many small clusters gives a qualitative idea of the heterogeneity of the dynamics at these temperatures.

7. Summary and conclusions

We describe the numerical solution of mean field equations and the implementation of Wolff cluster MC algorithm for a cell model for liquid water. The mean field approach allows us to estimate in an approximate way the phase diagram of the model at any state point predicting intriguing new results at very low T [21].

To explore the state points of interest for these predictions the use of standard simulations, such as molecular dynamics or Metropolis MC, is not effective due to the onset of the glassy dynamics [8]. To overcome this problem and access the deeply supercooled region of liquid water, we adopt the Wolff cluster MC algorithm. This method, indeed, allows us to greatly accelerate the autocorrelation time of the system. Direct comparison of Wolff's dynamics with Metropolis dynamics in the vicinity of the liquid–liquid critical point shows a reduction of the autocorrelation time of a factor at least 10^4.

Furthermore, the analysis of the clusters generated during the Wolff MC dynamics allows to emphasize how the regions of tetrahedrally ordered molecules build up on approaching the liquid–liquid critical point, giving rise to the backbone of the tetrahedral hydrogen bond network at the phase transition [23]. The coexistence of clusters of correlated molecules with sizes that change

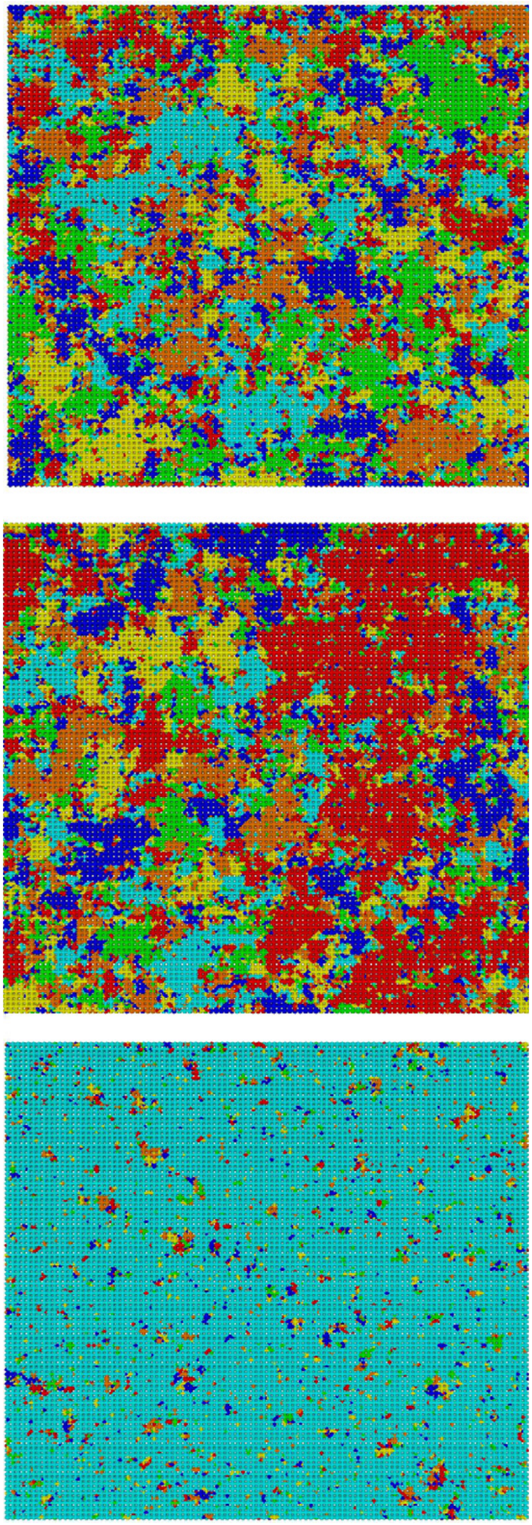

Fig. 4. Three snapshots of the system with $N = 100 \times 100$, showing the Wolff's clusters of correlated water molecules. For each molecule we show the states of the four arms and associate different colors to different arm's states. The state points are at pressure close to the critical value P_C ($Pv_0/\epsilon = 0.72 \simeq P_C v_0/\epsilon$) and $T > T_C$ (top panel, $k_B T/\epsilon = 0.0530$), $T \simeq T_C$ (middle panel, $k_B T/\epsilon = 0.0528$), $T < T_C$ (bottom panel, $k_B T/\epsilon = 0.0520$), showing the onset of the percolation at $T \simeq T_C$.

with the state point gives a rationale for the heterogeneous dynamics observed in supercooled water [22].

Acknowledgements

We thank Andrew Inglis for introducing one of the authors (M.G.M.) to VPython, Francesco Mallamace for discussions, NSF grant CHE0616489 and Spanish MEC grant FIS2007-61433 for support.

References

[1] G. Franzese, M. Rubi (Eds.), Aspects of Physical Biology: Biological Water, Protein Solutions, Transport and Replication, Lecture Notes in Physics, vol. 752, Springer, Berlin, 2008.

[2] P.G. Debenedetti, J. Phys.: Condens. Matter 15 (2003) R1669.

[3] P.G. Debenedetti, H.E. Stanley, The physics of supercooled and glassy water, Physics Today 56 (6) (2003) 40.

[4] G. Franzese, K. Stokely, X.-Q. Chu, P. Kumar, M.G. Mazza, S.-H. Chen, H.E. Stanley, J. Phys.: Condens. Matter 20 (2008) 494210.

[5] C.A. Angell, Science 319 (2008) 582.

[6] H.E. Stanley, P. Kumar, G. Franzese, L.M. Xu, Z.Y. Yan, M.G. Mazza, S.-H. Chen, F. Mallamace, S.V. Buldyrev, Liquid polyamorphism: Some unsolved puzzles of water in bulk, nanoconfined, and biological environments, in: M. Tokuyama, I. Oppenheim, H. Nishiyama (Eds.), Complex Systems, AIP Conference Proceedings 982 (2008) 251.

[7] H.E. Stanley, S.V. Buldyrev, G. Franzese, N. Giovambattista, F.W. Starr, Phil. Trans. Royal Soc. 363 (2005) 509;
P. Kumar, G. Franzese, S.V. Buldyrev, H.E. Stanley, Phys. Rev. E 73 (2006) 041505.

[8] P. Kumar, G. Franzese, H.E. Stanley, Phys. Rev. Lett. 100 (2008) 105701.

[9] U. Wolff, Phys. Rev. Lett. 62 (1989) 361.

[10] G. Franzese, H.E. Stanley, J. Phys.: Condens. Matter 14 (2002) 2201; Physica A 314 (2002) 508.

[11] K. Stokely, M.G. Mazza, H.E. Stanley, G. Franzese, Effect of hydrogen bond cooperativity on the behavior of water, arXiv:0805.3468v1, 2008.

[12] G. Franzese, H.E. Stanley, J. Phys.: Condens. Matter 19 (2007) 205126.

[13] P. Kumar, G. Franzese, H.E. Stanley, J. Phys.: Condens. Matter 20 (2008) 244114.

[14] G. Franzese, M.I. Marqués, H.E. Stanley, Phys. Rev. E 67 (2003) 011103.

[15] M.I. Marqués, Phys. Rev. E 76 (2007) 021503.

[16] M.A. Ricci, F. Bruni, A. Giuliani Similarities between confined and supercooled water, Faraday Discuss. 141 (2009) 347;
M. Chaplin, Water's hydrogen bond strength, cond-mat/0706.1355, 2007.

[17] The model does not differentiate “donor” molecule and “acceptor” molecule in the hydrogen bond definition. This simplification increases the number of possible bonded configurations, hence increases the entropy associated to the local tetrahedral configurations. A simple modification of the model could explicitly take into account this feature, however the comparison of the results from the present version of the model with experiments and simulations from more detailed models shows good qualitative agreement.

[18] V. Cataudella, G. Franzese, M. Nicodemi, A. Scala, A. Coniglio, Phys. Rev. E 54 (1996) 175;
G. Franzese, J. Phys. A 29 (1996) 7367.

[19] A. Coniglio, F. Peruggi, J. Phys. A 15 (1982) 1873.

[20] The results of [18,19] guarantee that the cluster algorithm described here satisfies the detailed balance and is ergodic. Therefore, it is a valid Monte Carlo dynamics.

[21] M.G. Mazza, K. Stokely, H.E. Stanley, G. Franzese, Anomalous specific heat of supercooled water, cond-mat/0807.4267, 2008.

[22] M.G. Mazza, et al., Phys. Rev. Lett. 96 (2006) 057803;
N. Giovambattista, et al., J. Phys. Chem. B 108 (2004) 6655;
M.G. Mazza, et al., Phys. Rev. E 76 (2007) 031203;
A.B. de Oliveira, P.A. Netz, M.C. Barbosa, Eur. Phys. J. B 64 (2008) 481.

[23] A. Oleinikova, I. Brovchenko, J. Phys.: Condens. Matter 18 (2006) S2247.